Identification of N7-methylguanosine-related patterns and characterization of the tumor microenvironment in hepatocellular carcinoma

Jianfa Yu
Tianjin First Center Hospital
Shuang Wang
Tianjin Central Hospital of Obstetrics and Gynecology
Rui Shi
Tianjin First Center Hospital
Long Yang
Tianjin First Center Hospital
Qi Lang
China Medical University
Yamin Zhang (yminzhang2219@163.com)
Tianjin First Center Hospital

Research Article

Keywords: N7-methylguanosine, Hepatocellular carcinoma, Tumor microenvironment, Prognosis

Posted Date: June 13th, 2022

DOI: https://doi.org/10.21203/rs.3.rs-1732234/v1

Abstract

Background: N7-methylguanosine (m7G) is an essential epigenetic modification and there is increasing evidence that it is closely associated with tumorigenesis progression. However, the expression pattern of m7G-related genes in hepatocellular carcinoma (HCC) remains systematically analyzed.

Methods: We downloaded HCC genetic and transcriptomic data from TCGA and GEO datasets. Unsupervised clustering methods identified different m7G-related gene subtypes, and then an m7G_score for predicting overall survival and characterizing the tumor microenvironment (TME) was constructed. Eventually, a highly accurate nomogram was constructed based on the score.

Results: In this study, two m7G-related gene subtypes were obtained by unsupervised clustering analysis of 18 m7G-related genes, and the relationship between different subtypes and clinicopathological features and TME was systematically evaluated.

Conclusion: N7-methylguanosine-related patterns are closely related to the clinical characteristics and tumor microenvironment of HCC patients, providing a new perspective on the treatment of HCC patients. Meanwhile, m7G_score can improve the clinical applicability with HCC patients.

1. Introduction

Primary liver cancer is the sixth most common cancer globally, of which hepatocellular carcinoma (HCC) accounts for 80%.[1,2] Early-stage HCC is mainly treated by surgical resection, and progressive stage HCC is treated by chemoembolization for local treatment, immunotherapy and targeted therapy for systemic treatment, etc. [3,4] However, even after treatment of early-stage HCC, the 5-year recurrence rate is still as high as 70%, so there is an urgent need to investigate the molecular mechanisms of hepatocellular carcinogenesis and develop targeted treatment strategies.[5]

The mechanism of HCC is complex and involves both the genetic and epigenetic levels.[6] There is much evidence linking dysregulated RNA modifications to the pathogenesis of human diseases, including cancers. More than 100 types of RNA modifications have been identified, and methylation modifications are one of the major forms of RNA modifications, accounting for about two-thirds of them.[7,8,9] N7-methylguanosine (m7G) is an essential epigenetic modification that plays a vital role in regulating gene expression. M7G is a modification that adds a methyl group to the seventh N position of RNA guanine by the action of methylation transferase. Studies have shown that m7G modifications are present in various molecules, including mRNA 5' cap structures, mRNA internal, pri-miRNA, transfer RNA (tRNA) and ribosomal RNA (rRNA).[10,11] There is growing evidence that impaired m7G tRNA modifications are associated with various diseases. For example, knockdown of METTL1 impairs m7G tRNA modification and induces abnormal differentiation and growth of embryonic stem cells.[12] Mutations in WDR4 result in different forms of small-headed primitive dwarfism.[13] These observations suggest a critical function for METTL1/WDR4-mediated m7G tRNA modifications in regulating cell fate determination and growth.

Recent studies have found that m7G is closely associated with tumorigeneses, such as METTL1 dysregulation associated with chemotherapy sensitivity in colon and cervical cancer cells,[14,15] METTL1/WDR4-mediated m7G tRNA modification and m7G codon use promoting mRNA translation and lung cancer progression[16] and METTL1 promoting hepatocarcinogenesis through m7G tRNA modification-dependent translational control.[17]

In this study, tumor immune microenvironment (TME) characteristics were systematically assessed in HCC patients by clustering the expression of previously studied m7G-related genes and m7G_score based on the differentially expressed genes (DEGs) of two m7G-related gene subtypes was used to predict survival and assess the immune landscape.

2. Materials And Methods

Data collection

TCGA-LIHC gene expression data (fragments per kilobase million, FPKM) and clinical data were obtained from The Cancer Genome Atlas (TCGA) (https://portal.gdc.cancer). HCC microarray expression dataset GSE14520 was obtained from Gene Expression Omnibus (GEO) (https://www.ncbi.nlm.nih.gov/geo). We transformed the FPKM data into transcripts per kilobase million (TPM) to make the RNA-seq data values closer to the microarray data and eliminated the batch effect by the "Combat" algorithm.[18]

Consensus clustering analysis of m7G-related genes

Eighteen m7G-related genes were obtained from MsigDB Team http://www.broad.mit.edu/gsea/msigdb/), and these genes were obtained in the supplementary material table S1. Based on the expression of these genes, the HCC samples were clustered unsupervised using the R package "ConsensusClusterPlus" to be classified into distinct molecular subtypes.[19] The optimal molecular subtypes were obtained by selecting the best K value. The Kaplan-Meier survival analysis was performed to assess the differences in survival between the distinct subtypes. Molecular subtypes were compared to assess differences between subtypes in terms of clinical characteristics. To investigate the activity of biological pathways in distinct molecular subtypes, Gene set variation analysis (GSVA) was performed using the hallmark gene set (c2.cp.kegg.v7.2) from the MsigMD database.[20] To examine the relative abundance of distinct subtypes of immune cells infiltration, the single-sample gene set enrichment analysis (ssGSEA)algorithm was performed in the R package "GSVA". In addition, the fraction of human immune cell subpopulations in 23 of each HCC sample was calculated by the CIBERSORT algorithm to compare the differences in the level of immune cell infiltration by molecular subtypes.[21]

Identification and enrichment analysis of DEGs

Distinct m7G subtype-related DEGs were identified using the "limma" package in R (*adj. p* < 0.05 and $|\log_2 FC|>1.5$).[22] The functional and enrichment pathways of DEGs were further explored using the

"clusterprofiler" package in R.[23]

Construction of prognostic m7G_score

The m7G subtype-related prognostic DEGs were identified using univariate Cox regression analysis. Patients were classified into distinct subtypes using Consensus clustering analysis based on these prognostic DEGs for deeper analysis. All HCC patients were divided into training and testing groups in a 1:1 ratio, then used training group to construct the prognostic m7G_score. Eventually, candidate genes were identified using lasso Cox regression analysis and multivariate Cox analysis. The m7G_score was constructed based on candidate genes with the formula:

M7G_score = Σ(Expi *Coefi)

Expi: Candidate gene expression value

Coefi: Candidate gene risk factor

Based on the median m7G_score, patients were divided into high-risk and low-risk groups, and the Kaplan-Meier survival analysis and receiver operating characteristic (ROC) curves were plotted to evaluate the merits of the model.

Validation by qRT-PCR and western blot

The total RNA was extracted using Trizol on ice (Thermo Fisher Scientific, Waltham, MA, USA) according to the manufacturer's instructions, and RNA purity and concentration were measured using a UV spectrophotometer. cDNA synthesis from RNA was performed using the RT-PCR kit (TAKARA047A; Takara bio, Shiga, Japan) of Super Script III First-Strand Synthesis System. The amplification conditions were: denaturation at 95°C for 30 s, 95°C for 5 s, and 60°C for 30 s, for a total of 40 cycles. Real-time PCR amplification was performed using the 7500 Fast Real-Time PCR system. The primers used for were shown in the supplementary material table S2. The tissues were lysed by chilled radio-immunoprecipitation assay (RIPA) and the bicinchoninic acid (BCA) method was used to determine the protein concentration of each lysate. Proteins (80 mg) were separated using 10% sodium dodecyl sulfate-polyacrylamide gel electrophoresis. The procedures were performed according to the manufacturer's protocol. The primary antibodies used were listed in the supplementary material table S3.

Relationship with TME of m7G_score

Using CIBERSORT to quantify the abundance of 23 infiltrating immune cells in samples from high and low-risk groups, we explored the m7G_score correlation with infiltrating immune cells. In addition, we assessed immune checkpoint expression between distinct groups.

Construction and validation of m7G_score nomogram

The nomogram was developed using the "rms" package in R.[24] The forecasting capability of the nomogram was evaluated using 1-year, 3-year and 5-year calibration curves.

Statistical analyses

All statistical analyses were performed using R version 4.1.0 and GraphPad Prism 8. Statistical significance was set at $P < 0.05$.

3. Results

Multi-omics analysis of m7G-related genes in HCC

The waterfall chart in the TCGA-LIHC somatic mutation dataset showed that m7G-related genes had lower mutation frequency, only mutating in 19 out of 364 samples (Fig. 1(a)). In the TCGA-LIHC somatic copy number dataset, copy number variants (CNV) were prevalent in m7G-related genes, with increased CNV in NCBP2 and LARP1 and decreased CNV in EIF4G3, EIF4E, DCPS and EIF4A1 (Fig. 1(b) and 1(c)). When comparing the gene expression in normal and tumor tissues, significant differences were found in the expression of 18 m7G-related genes, indicating that m7G-related gene expression plays a vital role in HCC (Fig. 1(d)). In addition, 15 m7G-related genes had significantly different survival curves(Fig. 2). It could be found that NCBP2 expression was significantly increased in HCC samples compared with normal samples, suggesting that the increased frequency of NCBP2 CNV may be one of the mechanisms of its overexpression, but it was not absolute. EIF4G3 CNV showed low frequency, but its expression was still higher in tumor samples than normal tissues. Therefore, the variation of CNV frequency is not the only factor affecting tumor gene expression.[25,26]

Identification of m7G-related gene subtypes in HCC

We integrated the TCGA-LIHC with the GSE14520 (GPL571) to examine the subtypes of HCC based on the expression of m7G-related genes. Then, Two m7G-related gene subtypes (subtype A and subtype B) were identified by unsupervised clustering (Fig. 3(a)). Principal component analysis (PCA) revealed significant differences in the transcriptional profiles of m7G-related genes between the two subtypes (Fig. 3(b)). In terms of survival analysis, Kaplan-Meier survival curves showed that subtype A had a significantly worse survival rate than subtype B (log-rank test, $p = 0.002$) (Fig. 3(c)). In terms of clinical clinicopathological features, the clinical TNM stages showed significant differences, and subtype A had a higher ratio of TNM stage III-IV than subtype B (Fig. 3(d)).

TME characteristics in m7G-related gene subtypes

To further explore the pathway enrichment characteristics of different subtypes of m7G-related genes, GSVA revealed that subtype A was significantly enriched in ubiquitin-mediated proteolysis and cell cycle(Fig. 4(a)). Ubiquitination modifications also play a vital role in the development of the human immune system and in the various stages of the immune response, such as the initiation, development

and conclusion of the immune response. Moreover, many ubiquitination modifications are able to suppress the immune response by degrading immunomodulatory proteins. To investigate the role of m7G-realted genes in TME of HCC, correlations between the two subtypes and 23 human immune cell subpopulations were assessed using the CIBERSORT algorithm, and the results suggested that the proportion of activated CD4 T infiltration was significantly higher in the A subtype than in the B subtype(Fig. 4(b)).

Identification of DEGs in m7G-related gene subtypes

To further explore the heterogeneity of m7G-related gene subtypes, we identified 1581 DEGs. Gene ontology (GO) and Kyoto Encyclopedia of Genes and Genomes (KEGG) analyses showed that these DEGs were significantly enriched in DNA replication biological processes and significantly enriched in cell cycle pathways(Fig. 5(a) and 5(b)). The prognostic value of 1134 subtype-associated genes was determined by univariate Cox regression analysis. A consensus clustering algorithm was used to validate this regulatory mechanism further, and classify patients into three gene subtypes (gene subtype A, gene subtype B and gene subtype C) based on 1134 subtype-associated genes. Kaplan-Meier curves showed that gene subtype C had the worst overall survival, while gene subtype B had a favorable overall survival(Fig. 5(c)). Furthermore, the three gene subtypes differed significantly in the expression of m7G-related genes(Fig. 5(d)).

Construction and validation of m7G_score

The best prognostic features were identified by lasso regression analysis and multivariate Cox regression analysis of 1134 subtype-associated genes, and eventually, five candidate genes (UCK2, PRKCD, UGT2B15, ADM, NQO1) were finally screened. The m7G_score formula was as follows:

m7G_score = (0.4466*expression of UCK2) +(0.2772* expression of PRKCD)+(-0.0928* expression of UGT2B15)+(0.2021* expression of ADM)+(0.0960* expression of NQO1)

Sankey diagram illustrated the distribution of m7G-related gene subtypes, gene subtypes and m7G_score groups(Fig. 6(a)). In comparing the m7G_score of m7G-related gene subtypes, it was found that the m7G_score of subtype A was significantly higher than that of subtype B(Fig. 6(b)). When comparing m7G_scores between gene subtypes, gene subtype C had the highest m7G_scores(Fig. 6(c)). When the m7G_scores were divided into two groups of high and low risk by median, the risk distribution graph showed that the survival time decreased significantly with increasing scores(Fig. 6(d)). In addition, Kaplan-Meier survival curves showed that the survival rate in the high-risk group was significantly lower than that in the low-risk group. In addition, the 1-year, 3-year, and 5-year survival rates for the m7G_score were expressed as area under the curve (AUC) of 0.754, 0.742, and 0.730, respectively(Fig. 6(d)).

Validation of Transcriptional level and expression level of five subtype-related prognostic genes in m7G_score

Five pairs of liver tissues (tumor tissues vs. adjacent normal tissues) were examined by qRT-PCR, and the results showed that ADM, UCK2, PRKCD and NOQ1 were transcribed at higher levels in liver cancer tissues than in adjacent normal tissues, while UGT2B15 was lower than in normal tissues(Fig. 7(c)). The expression levels of ADM, UCK2, PRKCD, NOQ1 and UGT2B15 in four pairs of liver tissues (tumor tissues vs. adjacent normal tissues) were detected by western blot, and the results were consistent with the transcriptional levels of each gene(Fig. 7(a) and 7(b)). In addition, we further explored the prognostic value of these genes by Kaplan-Meier Plotter website, which showed that high expression of ADM, UCK2, PRKCD and NOQ1 was associated with shorter OS (P = 0.0081, P = 1.3e-09, P = 0.00036 and P = 0.001, respectively), while low expression of UGT2B15 was associated with worse prognosis (P = 0.0022) (Fig. 7(d)).[27]

Relationship between m7G_score and TME

The relationship between m7G_score and immune cell abundance was positively correlated with T cell regulatory and negatively correlated with T cells CD4 memory by the CIBERSORT algorithm(Fig. 8(a)). We evaluated the relationship between five candidate genes and immune cell abundance, and the heat map showed that these genes were significantly associated with multiple immune cells(Fig. 8(b)). In addition, immune checkpoint expression was significantly higher in the high-risk group than in the low-risk group(Fig. 8(c)).

Constructing nomograms to predict survival

We combined m7G_score and TNM stage as predictors to construct a nomogram, through which we could better show the survival rate of patients at 1, 3 and 5 years(Fig. 9(a)). The calibration curves showed that the predicted survival at 1, 3 and 5 years was very similar to the actual survival, reflecting an excellent predictive efficacy(Fig. 9(b)).

4. Discussion

HCC remains a global health challenge and its incidence continues to increase year by year. HCC is the most common form of liver cancer and the molecular mechanisms depending on different genotoxic insults and risk factors. Although we now have a relatively new understanding of the physiopathology and mechanistic studies of HCC, we still face challenges in clinical translation.

Genetic and epigenetic misregulation is a critical mechanistic factor in the development and progression of HCC. Methylation is one of the most common modifications of RNA, and RNA methylation has been shown to be associated with a variety of human diseases, with aberrant methylation leading to disease and cancer, particularly in tumors.[28] Compared to mRNA, tRNA modifications are more widespread. The tRNA modification can regulate tRNA stability, mRNA translation and protein synthesis rates, and mutations or dysregulated expression of tRNA-modified enzymes which have been widely observed in human diseases. [29,30,31]However, in cancers, the physiological functions of tRNA modifications are poorly understood. The m7G is one of the most prevalent tRNA modifications in the tRNA variable loop.

However, the oncogenic functions and potential mechanisms of m7G tRNA modifications in cancer have not been fully elucidated. Recent studies have found that m7G tRNA modifications have effects on a variety of cancers, such as HCC, intrahepatic cholangiocarcinoma, lung cancer, bladder cancer, Esophageal Cancer, etc[17,32,33,16,34,35]

In this study, the overall alterations of m7G-related genes in HCC at the gene level and expression level were revealed by 18 m7G-related genes. The results showed that the mutation level of these genes in HCC was not high, only 5.22% of the mutation frequency, and the CNV results showed that the loss of EIF4G3 CNV was the most, higher than 15%, but the transcriptional level was found to be higher in the tumor than the normal group. It is commonly believed that CNV loss causes a decrease in transcript levels, but transcript levels are affected not only by CNV but also by DNA methylation, transcription factors, and other factors. [25,26] In the transcribed landscape, these 18m7G-related genes were significantly different in both tumor tissues and normal tissues, suggesting that m7G-related genes play an important role in HCC development. We identified two molecular subtypes based on 18 m7G-related genes, and result showed that patients with subtype A had worse overall survival and clinical staging than patients with subtype B. GSVA revealed that subtype A was characterized by a significant enrichment in cell cycle, ubiquitin-mediated protein degradation pathways, suggesting a higher degree of tumor progression in patients with subtype A. In addition, immune cell tumor infiltration of both molecular subtypes existed to varying degrees in CD4 T and NK cells. To better reveal the differences that existed between the two molecular subtypes, GO and KEGG enrichment was performed by identifying mRNA expression differences and based on DEGs that were shown to be significantly enriched in DNA replication and cell cycle checkpoint. We finally obtained 5 candidate genes based on these genes by unvariate analysis, lasso regression analysis, and multivariate analysis, and constructed m7G_score to predict survival based on these 5 genes, that was demonstrated its strong predictive ability for prognostic survival.

Usually, a solid and effective immune system plays a crucial role in the fight against tumorigenesis and progression. [36]Among them, immune cells play an essential role in the tumor microenvironment, including innate immune cells (neutrophils, dendritic cells, macrophages, NK cells, etc.) and adaptive immune cells (T cells and B cells).[37] However, tumors can escape from the immune system by a variety of means, contributing to the phenomenon of immune escape. [38,39] We observed that T cell CD4 memory activation, T cell regulation (Treg), and macrophage M0 were positively correlated with a risk score, while T cells gamma delta, mast cells, and macrophage M1 were negatively correlated with a risk score. It was shown that increased numbers of Treg cells in the tumor microenvironment and the ability to attenuate effector T cells suppressed tumor immunity,[40,41]and that T cells gamma delta effectively-recognized and killed tumor cells, thereby regulating multiple mechanisms to inhibit tumor progression.[42]The high m7G_score group exhibited immunosuppressive features and T cell regulatory were associated with high m7G_score, while T cells gamma delta were associated with low m7G_score, again suggesting that the subtype A is immunosuppressive, having a poorer prognosis and lower immunogenicity, which was similarly validated by the fact that multiple immune checkpoints were higher in the high m7G_score

group than in the low m7G_score group. It indicates that molecular subtypes constructed using m7G-related genes can provide new insights in immunotherapy.

Finally, by integrating the m7G_score and TNM staging, we established a quantitative nomogram, which further improved the performance and facilitated the use of the m7G_score. This prognostic model can be used to stratify HCC patients' prognosis, help understand the molecular mechanisms of HCC better and provide new ideas for comprehensive treatment.

5. Conclusion

We identified two subtypes with different clinical and immunological characteristics in HCC by m7G-related genes. The comprehensive analysis revealed a wide range of regulatory mechanisms affecting tumor clinicopathological characteristics, tumor microenvironment and prognosis, which provides new ideas to guide personalized treatment strategies for HCC patients.

Declarations

Data Availability

The data used to support the findings of this study are available from the corresponding authors on reasonable request.

Conflicts of Interest

The authors declare that they have no conflicts of interest.

Authors' Contributions

Yamin Zhang and Jianfa Yu participated sufficiently in conception and design of study . Shuang Wang and Rui Shi carried out t data curation. Qi Lang and Long Yang was involved in data analysis. All authors read and approved the submitted manuscript.

Acknowledgments

Healthcare Science and Technology Project of Tianjin Municipality(ZC20064)

References

1. Llovet, J. M. *et al.* Hepatocellular carcinoma. Nat. Rev. Dis. Prim. **7**, (2021).
2. Pérez, L. M., López, S. A., Fajes, J. L. H. & Martín, L. C. Hepatocellular carcinoma. Med. (2020) doi:10.1016/j.med.2020.06.019.
3. Angeli, P., Bernardi, M. & Villanueva, C. European Association for the Study of the Liver. EASL Clinical Practice Guidelines for the management of patients with decompensated cirrhosis. J Hepatol.

(2018).

4. Llovet, J. M. *et al.* Trial Design and Endpoints in Hepatocellular Carcinoma: AASLD Consensus Conference. *Hepatology* (2021) doi:10.1002/hep.31327.
5. Roayaie, S. *et al.* The role of hepatic resection in the treatment of hepatocellular cancer. Hepatology (2015) doi:10.1002/hep.27745.
6. Dawson, M. A. & Kouzarides, T. Cancer epigenetics: From mechanism to therapy. Cell (2012) doi:10.1016/j.cell.2012.06.013.
7. Zhang, S. Mechanism of N 6 -methyladenosine modification and its emerging role in cancer. Pharmacology and Therapeutics (2018) doi:10.1016/j.pharmthera.2018.04.011.
8. Wood, S., Willbanks, A. & Cheng, J. X. The Role of RNA Modifications and RNA-modifying Proteins in Cancer Therapy and Drug Resistance. Curr. Cancer Drug Targets (2021) doi:10.2174/1568009621666210127092828.
9. Jonkhout, N. *et al.* The RNA modification landscape in human disease. RNA (2017) doi:10.1261/rna.063503.117.
10. Song, B. *et al.* M7GHub: Deciphering the location, regulation and pathogenesis of internal mRNA N7-methylguanosine (m7G) sites in human. Bioinformatics (2020) doi:10.1093/bioinformatics/btaa178.
11. Pandolfini, L. *et al.* METTL1 Promotes let-7 MicroRNA Processing via m7G Methylation. Mol. Cell (2019) doi:10.1016/j.molcel.2019.03.040.
12. Lin, S. *et al.* Mettl1/Wdr4-Mediated m 7 G tRNA Methylome Is Required for Normal mRNA Translation and Embryonic Stem Cell Self-Renewal and Differentiation. Mol. Cell (2018) doi:10.1016/j.molcel.2018.06.001.
13. Shaheen, R. *et al.* Mutation in WDR4 impairs tRNA m7G46 methylation and causes a distinct form of microcephalic primordial dwarfism. Genome Biol. (2015) doi:10.1186/s13059-015-0779-x.
14. Liu, Y. *et al.* Overexpressed methyltransferase-like 1 (METTL1) increased chemosensitivity of colon cancer cells to cisplatin by regulating miR-149-3p/S100A4/p53 axis. Aging (Albany. NY). (2019) doi:10.18632/aging.102575.
15. Okamoto, M. *et al.* tRNA Modifying Enzymes, NSUN2 and METTL1, Determine Sensitivity to 5-Fluorouracil in HeLa Cells. PLoS Genet. (2014) doi:10.1371/journal.pgen.1004639.
16. Ma, J. *et al.* METTL1/WDR4-mediated m7G tRNA modifications and m7G codon usage promote mRNA translation and lung cancer progression. Mol. Ther. **29**, 3422–3435 (2021).
17. Chen, Z. *et al.* METTL1 promotes hepatocarcinogenesis via m 7 G tRNA modification-dependent translation control. Clin. Transl. Med. **11**, (2021).
18. Zhao, Y. *et al.* TPM, FPKM, or Normalized Counts? A Comparative Study of Quantification Measures for the Analysis of RNA-seq Data from the NCI Patient-Derived Models Repository. J. Transl. Med. (2021) doi:10.1186/s12967-021-02936-w.
19. Wilkerson, M. D. & Hayes, D. N. ConsensusClusterPlus: A class discovery tool with confidence assessments and item tracking. Bioinformatics (2010) doi:10.1093/bioinformatics/btq170.

20. Hänzelmann, S., Castelo, R. & Guinney, J. GSVA: Gene set variation analysis for microarray and RNA-Seq data. BMC Bioinformatics (2013) doi:10.1186/1471-2105-14-7.
21. Newman, A. M. *et al.* Robust enumeration of cell subsets from tissue expression profiles. Nat. Methods (2015) doi:10.1038/nmeth.3337.
22. Ritchie, M. E. *et al.* Limma powers differential expression analyses for RNA-sequencing and microarray studies. Nucleic Acids Res. (2015) doi:10.1093/nar/gkv007.
23. Yu, G., Wang, L. G., Han, Y. & He, Q. Y. ClusterProfiler: An R package for comparing biological themes among gene clusters. Omi. A J. Integr. Biol. (2012) doi:10.1089/omi.2011.0118.
24. Iasonos, A., Schrag, D., Raj, G. V. & Panageas, K. S. How to build and interpret a nomogram for cancer prognosis. Journal of Clinical Oncology (2008) doi:10.1200/JCO.2007.13.5913.
25. Koch, A. *et al.* Analysis of DNA methylation in cancer: Location revisited. Nature Reviews Clinical Oncology (2018) doi:10.1038/s41571-018-0004-4.
26. Lambert, S. A. *et al.* The Human Transcription Factors. Cell (2018) doi:10.1016/j.cell.2018.01.029.
27. Menyhárt O, Nagy Á, Győrffy B. Determining consistent prognostic biomarkers of overall survival and vascular invasion in hepatocellular carcinoma. R Soc Open Sci. 2018;5(12):181006. doi:10.1098/rsos.181006
28. Delaunay, S. & Frye, M. RNA modifications regulating cell fate in cancer. Nature Cell Biology (2019) doi:10.1038/s41556-019-0319-0.
29. Tomikawa, C. 7-methylguanosine modifications in transfer RNA (tRNA). International Journal of Molecular Sciences (2018) doi:10.3390/ijms19124080.
30. Wiener, D. & Schwartz, S. The epitranscriptome beyond m6A. Nature Reviews Genetics (2021) doi:10.1038/s41576-020-00295-8.
31. Motorin, Y. & Helm, M. Methods for RNA modification mapping using deep sequencing: Established and new emerging technologies. Genes (2019) doi:10.3390/genes10010035.
32. Xia, P. *et al.* MYC-targeted WDR4 promotes proliferation, metastasis, and sorafenib resistance by inducing CCNB1 translation in hepatocellular carcinoma. Cell Death Dis. **12**, 1–14 (2021).
33. Dai, Z. *et al.* N7-Methylguanosine tRNA modification enhances oncogenic mRNA translation and promotes intrahepatic cholangiocarcinoma progression. Mol. Cell **81**, 3339–3355.e8 (2021).
34. Ying, X. *et al.* METTL1-m 7 G-EGFR/EFEMP1 axis promotes the bladder cancer development. Clin. Transl. Med. **11**, (2021).
35. Han, H. *et al.* N7-methylguanosine tRNA modification promotes esophageal squamous cell carcinoma tumorigenesis via the RPTOR/ULK1/autophagy axis. Nat. Commun. (2022) doi:10.1038/s41467-022-29125-7.
36. Wu, T. & Dai, Y. Tumor microenvironment and therapeutic response. Cancer Letters (2017) doi:10.1016/j.canlet.2016.01.043.
37. Hinshaw, D. C. & Shevde, L. A. The tumor microenvironment innately modulates cancer progression. Cancer Research (2019) doi:10.1158/0008-5472.CAN-18-3962.

38. Chen, Y. & Tian, Z. HBV-induced immune imbalance in the development of HCC. Frontiers in Immunology (2019) doi:10.3389/fimmu.2019.02048.
39. Ruf, B., Heinrich, B. & Greten, T. F. Immunobiology and immunotherapy of HCC: spotlight on innate and innate-like immune cells. Cellular and Molecular Immunology (2021) doi:10.1038/s41423-020-00572-w.
40. Najafi, S. & Mirshafiey, A. The role of T helper 17 and regulatory T cells in tumor microenvironment. Immunopharmacology and Immunotoxicology (2019) doi:10.1080/08923973.2019.1566925.
41. Huppert, L. A. *et al.* Tissue-specific Tregs in cancer metastasis: opportunities for precision immunotherapy. Cellular and Molecular Immunology (2022) doi:10.1038/s41423-021-00742-4.
42. Ma, R., Yuan, D., Guo, Y., Yan, R. & Li, K. Immune Effects of γδ T Cells in Colorectal Cancer: A Review. Frontiers in Immunology (2020) doi:10.3389/fimmu.2020.01600.

Figures

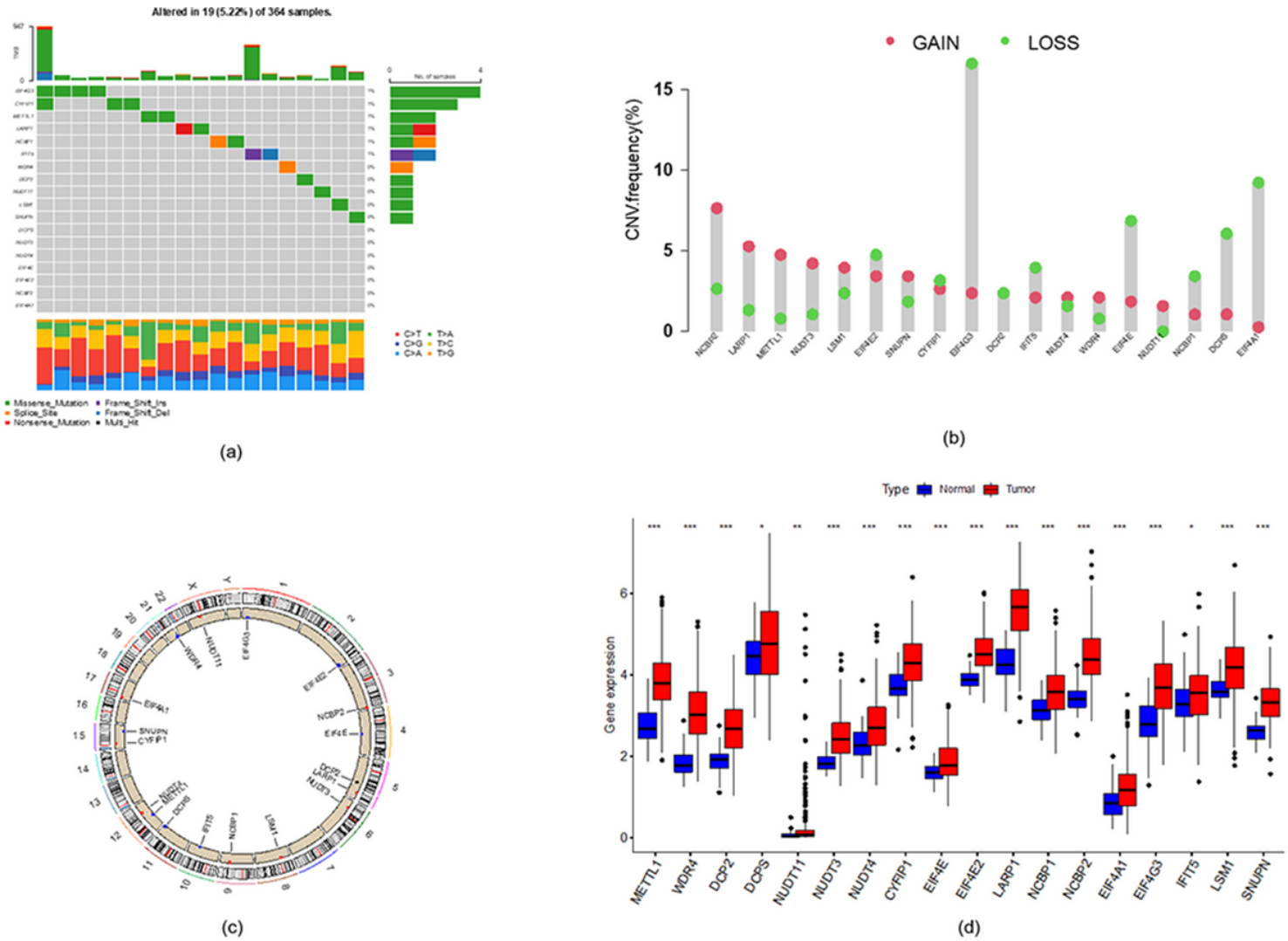

Figure 1

Genetic and transcriptional alterations of m7G-related genes in HCC. (a) Mutation frequencies of eighteen m7G-related genes from the TCGA-LIHC cohort. (b) Frequency of CNV in m7G-related genes. (c) Location of CNV alterations in m7G-related genes on twenty-three chromosomes. (d) Expression distributions of eighteen m7G-related genes between normal and HCC tissues. HCC, hepatocellular carcinoma; CNV, copy number variant.

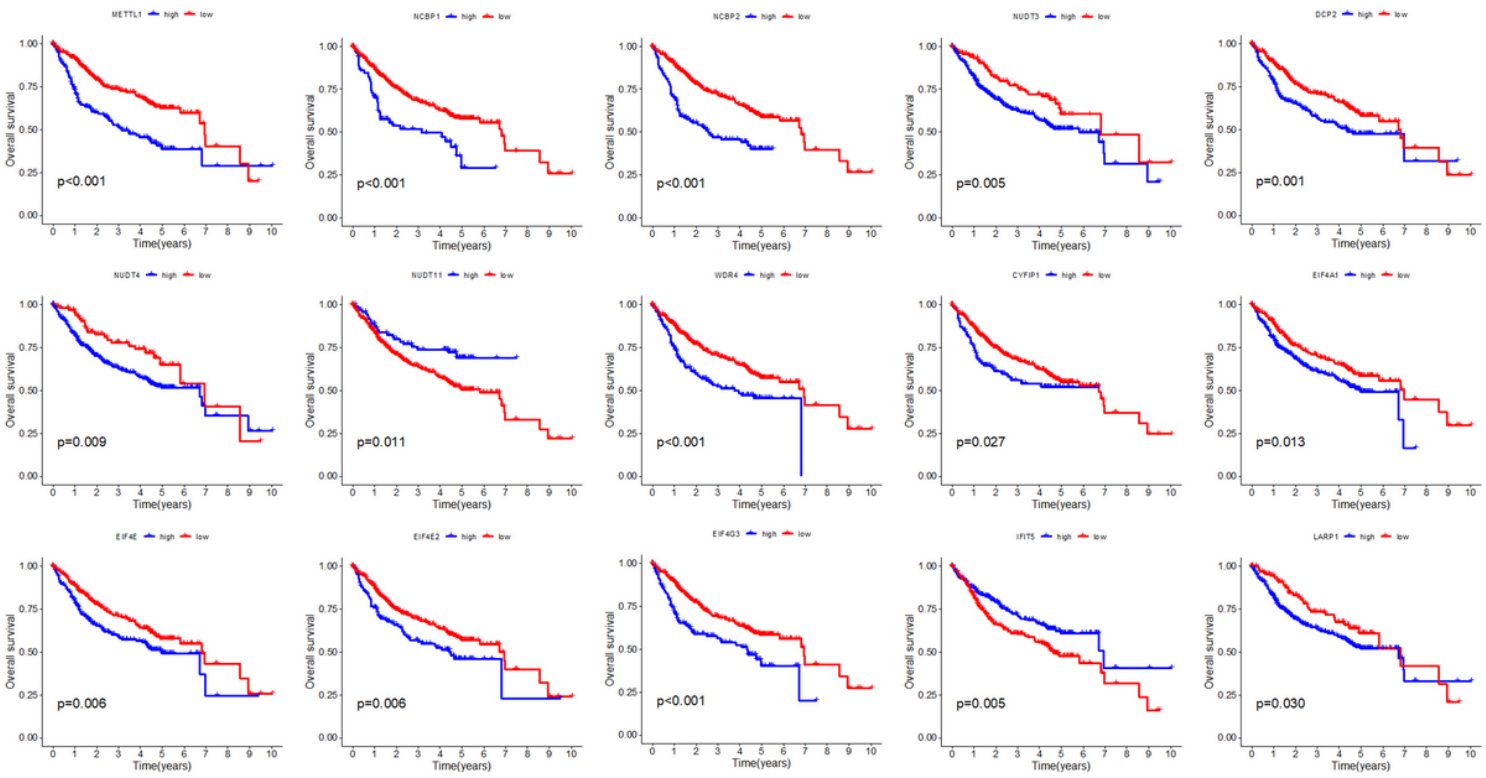

Figure 2

Fifteen m7G-related genes with significant survival differences.

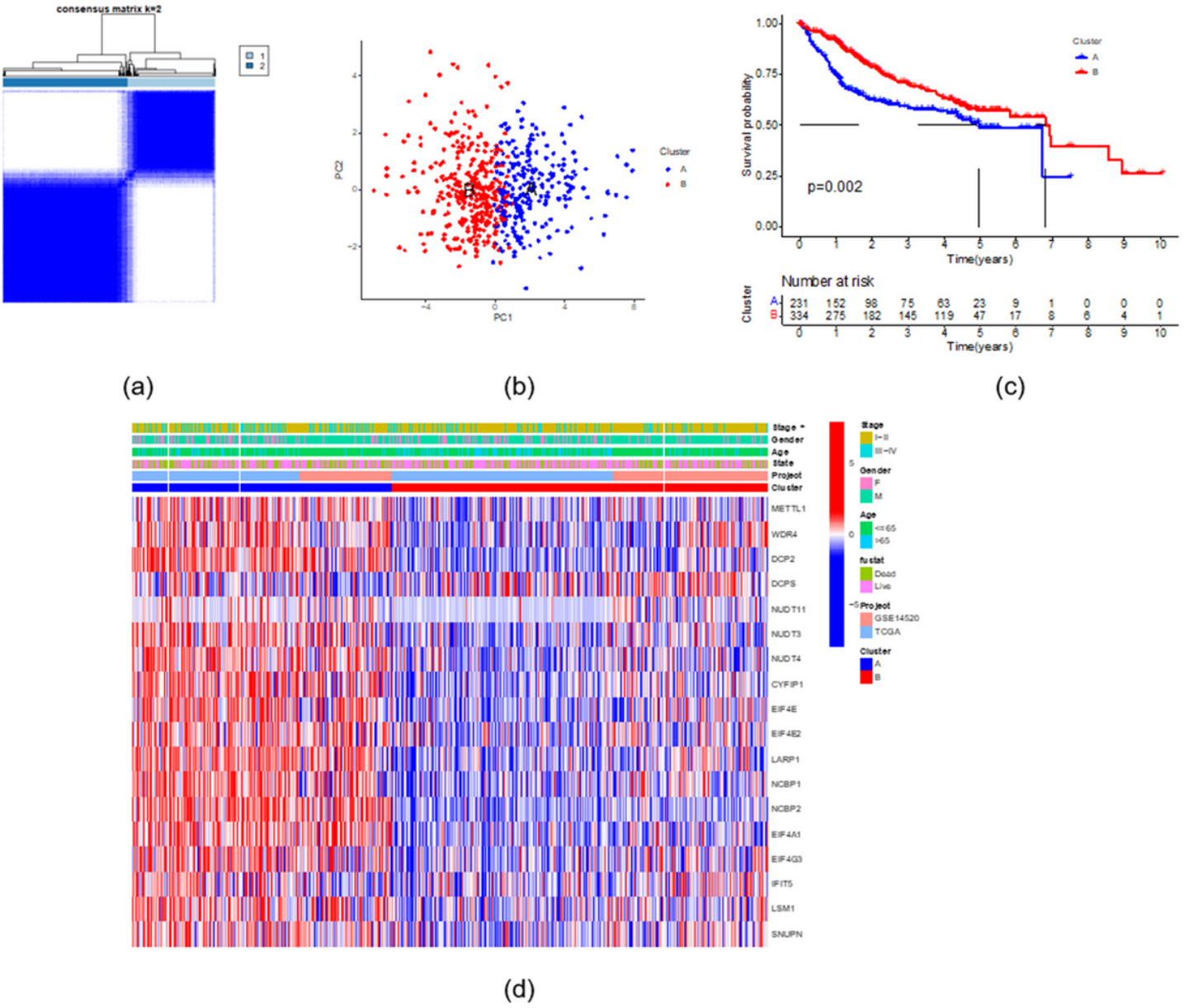

Figure 3

Characteristics of two m7G-related genes subtypes obtained by unsupervised clustering analysis. (a) Consensus matrix heatmap defining two clusters (k = 2). (b) PCA analysis revealed differences in the transcriptomes of the two m7G-related gene subtypes. (c) Survival analysis for two m7G-related genes subtypes. (d) Clinicopathological characteristics and expression differences between the two m7G-related genes subtypes.

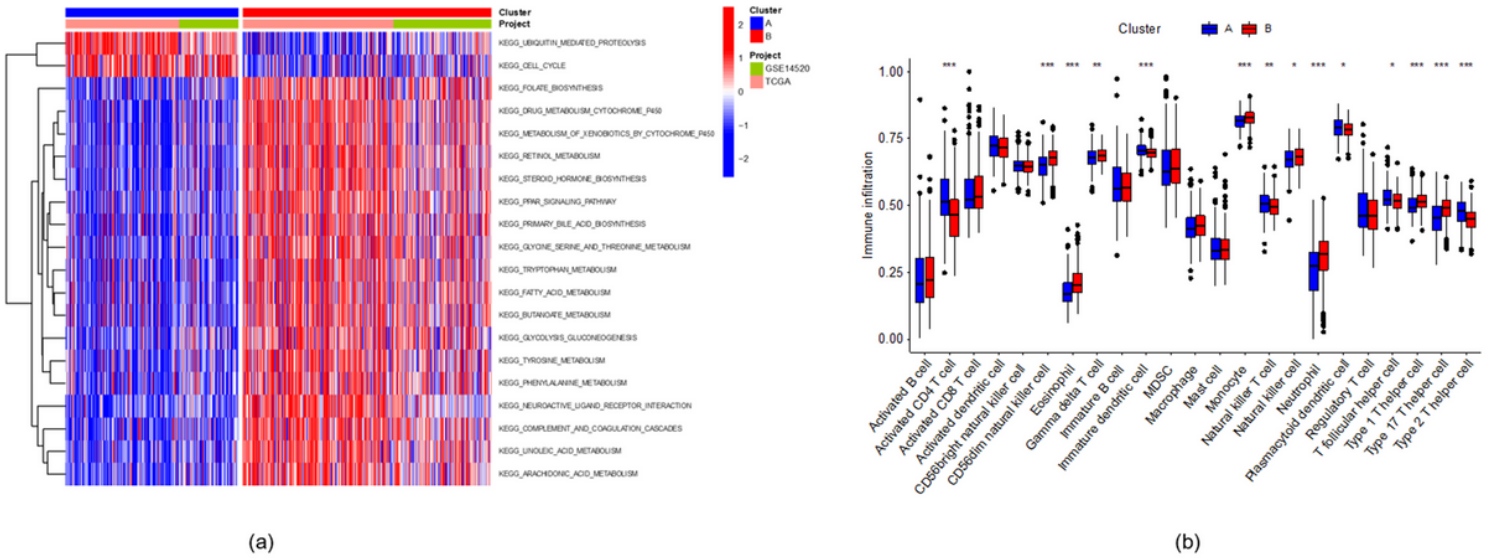

Figure 4

Correlation of two m7G-related genes subtypes of HCC and TME. (a) GSVA of a biological pathway between two m7G-related genes subtypes. (b) An abundance of 23 infiltrating immune cells in two m7G-related genes subtypes. HCC, hepatocellular carcinoma; TME, tumor microenvironment; GSVA, gene set variation analysis.

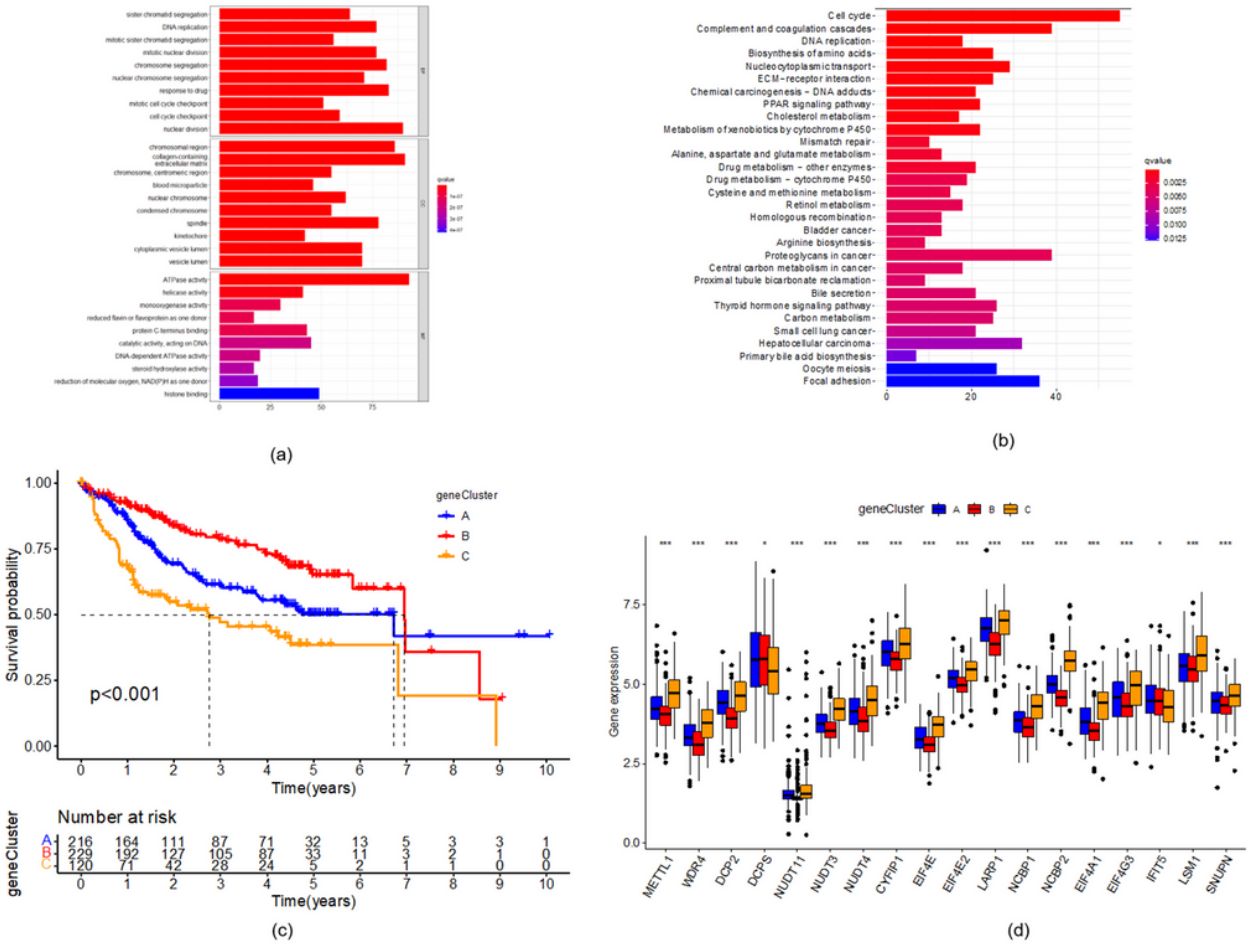

Figure 5

Identification of gene subtypes based on DEGs. (a) GO and KEGG enrichment analysis of DEGs among two m7G-related gene subtypes. (b) Kaplan-Meier curves for the three gene subtypes. (c) Differences in the expression of eighteen m7G-related genes between three gene subtypes.

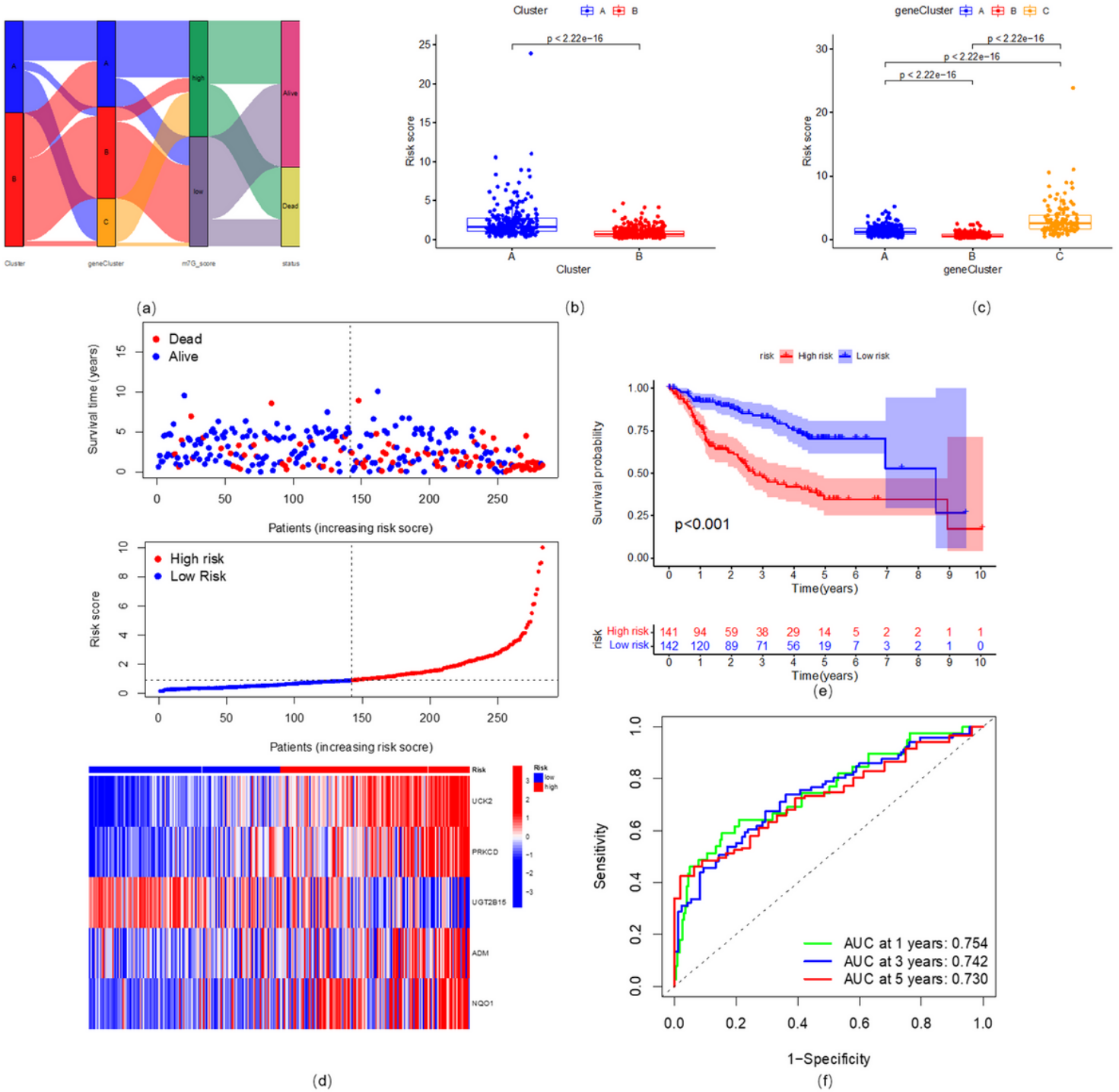

Figure 6

Characteristic of m7G_score. (a) Alluvial diagram of subtype distributions with m7G_score and survival status. (b) Differences in m7G_score between distinct m7G-related genes subtypes. (c) Differences in m7G_score between distinct gene subtypes. (d) The ranked dot plot, scatter plot and heatmap of m7G_score distribution in training group, (e) Survival analysis between the high- and low-risk group in training group. (f)ROC curves to predict the sensitivity and specificity of 1-, 3-, and 5-year survival according to the m7G_score in training group.

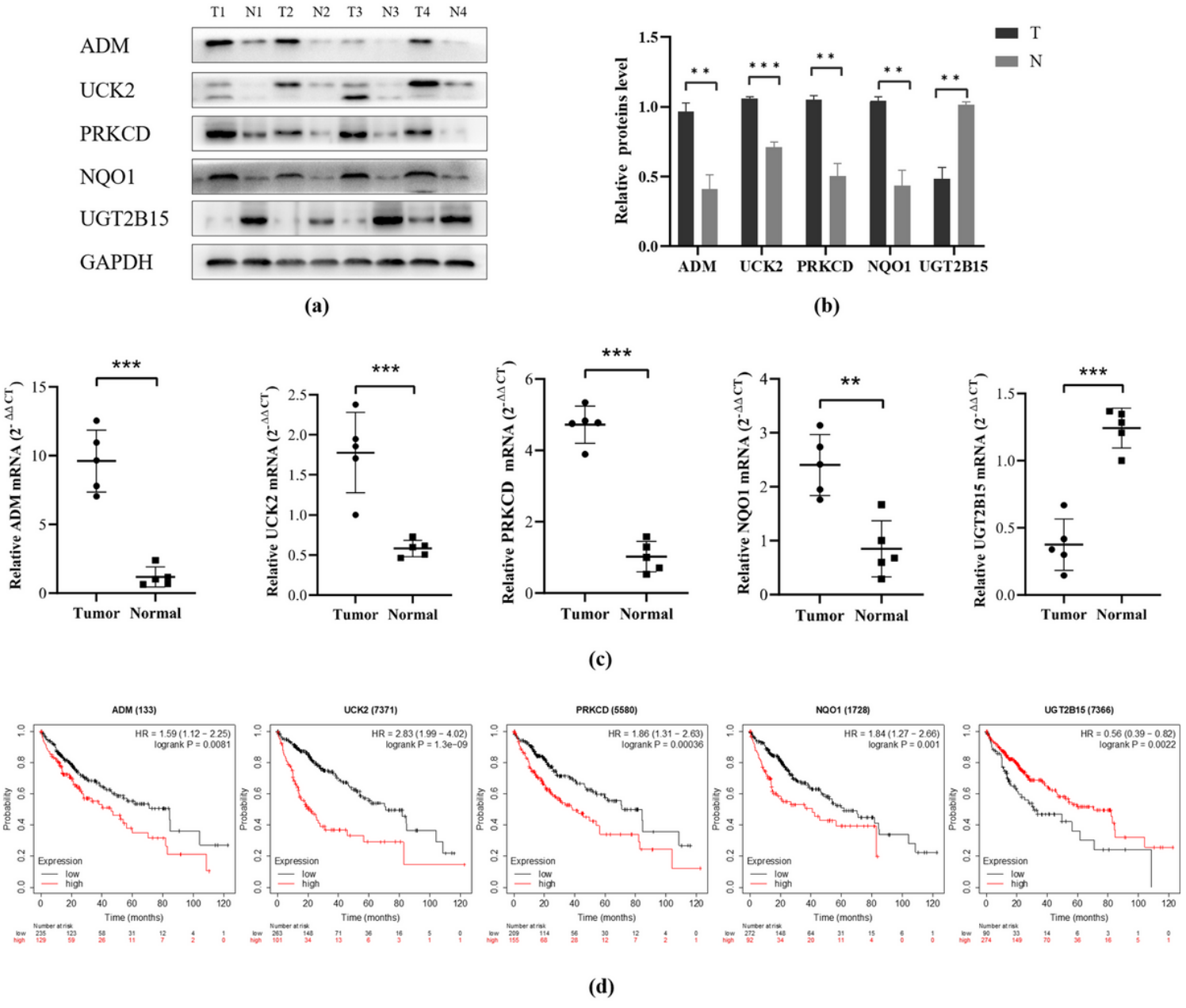

Figure 7

Western blot and qRT-PCR results of subtype-related prognostic genes. (a) Expression of ADM, UCK2, PRKCD, NQO1 and UGT2B15 in tissues by western blotting (n =4 for each group). (b) Relative values of ADM, UCK2, PRKCD, NQO1 and UGT2B15 in the tissues mentioned in (a), GAPDH was as the internal control. (c) The mRNA expression of ADM, UCK2, PRKCD, NQO1 and UGT2B15 in liver tissue samples by

qRT-PCR (2-ΔΔCт□□n=5□.(d). Prognostic values of dysregulated ADM, UCK2, PRKCD, NQO1 and UGT2B15 in liver tissues, as analyzed by Kaplan-Meier Plotter. Data are presented as mean ± SD.*, P < 0.05; **, P < 0.01; ***, P < 0.001.

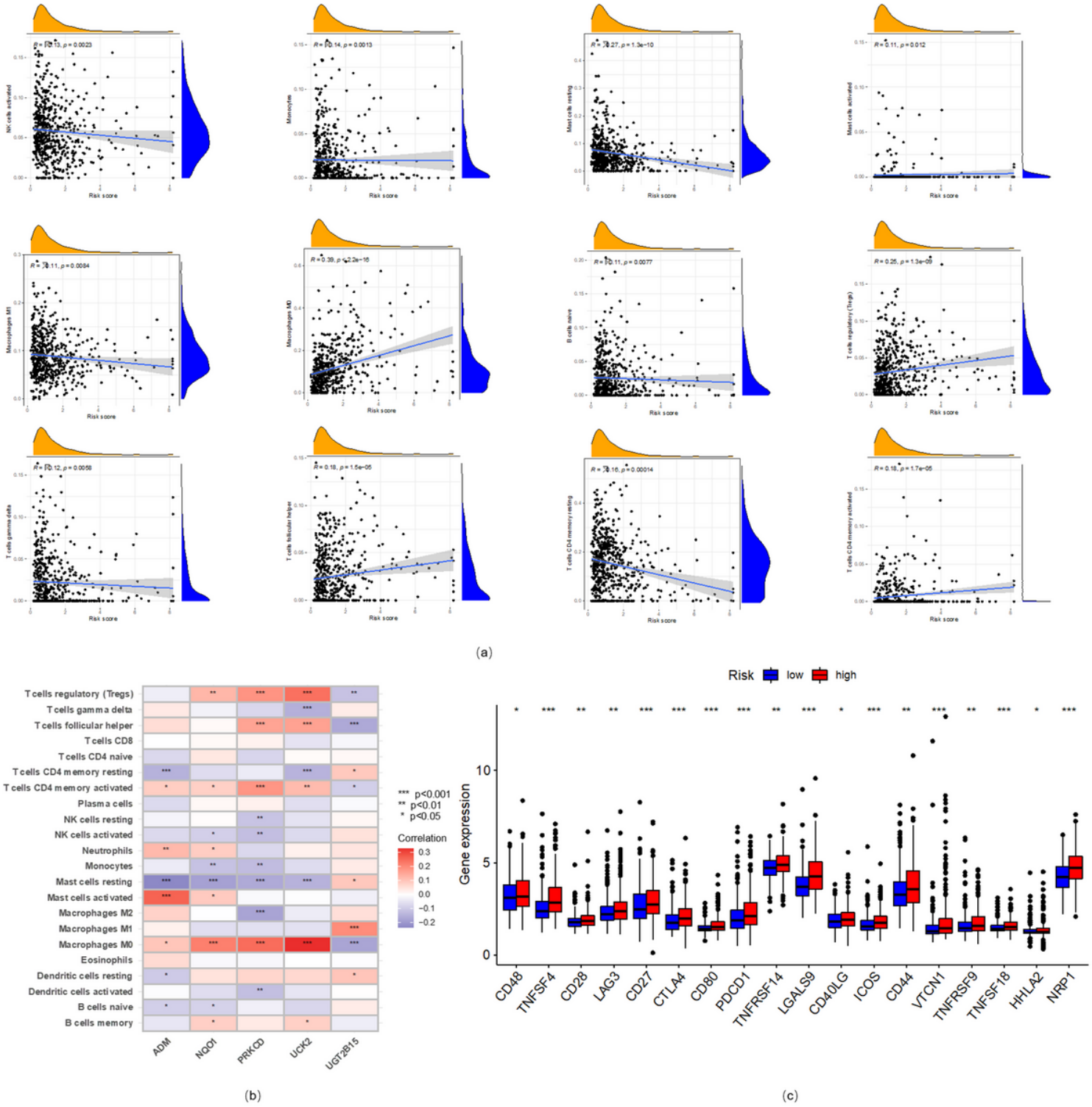

Figure 8

Evaluation of TME and immune checkpoints in both groups. (a) Correlation between m7G_score and immune cell types. (b) Correlation between immune cell abundance and five genes in m7g_score model.

(c) Expression of immune checkpoints in both groups. TME, tumor microenvironment.

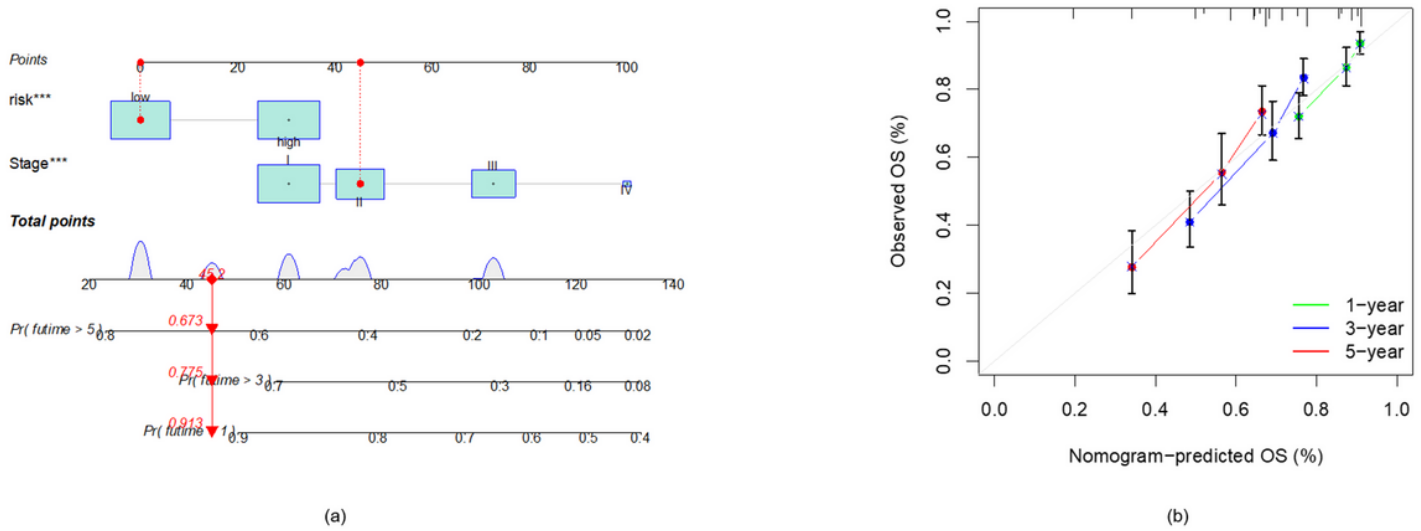

Figure 9

Construction of a nomogram. (a) Nomogram for predicting 1-, 3-, and 5-year survival in HCC patients. (b) Calibration curves for the nomogram were used to predict 1-, 3-, and 5-year survival.

Supplementary Files

This is a list of supplementary files associated with this preprint. Click to download.

- Supplementaryfiles.docx